ADVANCED INTELLIGENT SYSTEMS
Open Access
www.advintellsyst.com

An Ultrathin and Lightweight Soft Inflatable Actuator for Natural Tactile Sensory Feedback

*Hanna Scherer, Francesco Iberite, Giulia Caserta, Nicolo Boccardo, Jacopo Carpaneto, Emanuele Gruppioni, Silvestro Micera, and Tommaso Proietti**

The human sense of touch converts skin deformations into electrical impulses, enabling functional tasks such as object recognition and manipulation. Providing haptic information is crucial for improving usability in applications like prosthetics. Soft actuators have the potential to deliver modality-matched feedback and high compression forces in a compact form. However, their full potential has been partially demonstrated. This study presents a soft inflatable actuator utilizing thermoplastic polyurethane to provide rich multimodal sensory feedback, including pressure and vibration. The actuator weighs less than 2 g and is 0.4 mm thick, significantly improving upon previous designs. Mechanical characterization reveals that the actuator can produce high-bandwidth vibrations (200 Hz) and high forces (28 Newtons at 60 kPa). Psychometric tests, conducted with 14 able-bodied individuals and three transradial amputees, show performance comparable to state-of-the-art invasive and noninvasive solutions (Weber constants within 0.19–0.22). Additionally, the actuator successfully provides different artificial roughness sensations in able-bodied individuals. Finally, amputees achieve an overall accuracy of 73.3% in a classification task, with dominant sensations of touch and pressure (45% of the stimuli). These results demonstrate that the proposed soft feedback actuator is effective, versatile, and lightweight, with potential for integration into robotic systems for feedback restoration and augmentation.

1. Introduction

The somatosensory system plays a crucial role in human interaction with the surrounding environment, enabling proprioception and perception of texture, surface properties, pressure, temperature changes, and pain.[1] This system is essential for somatosensory guidance, significantly enhancing precise motor control and coordination. The absence of sensory feedback strongly reduces user performance and engagement in a wide range of applications including surgical robotics,[2] teleoperation,[3] and virtual reality[4] impacting the overall functionality and usability. The impact is even more severe in individuals with sensory impairments, such as amputees,[5] stroke survivors, and patients with spinal cord injuries.[6] In the former case, artificial haptic feedback can augment and substitute for the lack of sensory information, while in the latter, it aims to restore essential sensory functions.[6]

The variety of applications for artificial haptic feedback has led to the development of systems that can deliver precise mechanical stimulation in a closed-loop manner. Various approaches have been used to provide haptic stimuli, including pressure,[7,8] vibration,[9,10] skin stretch,[11,12] squeeze,[13,14] electrical,[15,16] and thermal[17,18] feedback. Although the goal of these systems is clear—replicating or restoring realistic sensations that allow the user to intuitively comprehend sensory information while being comfortable, wearable, and affordable—remains an ongoing challenge.[19]

H. Scherer, F. Iberite, J. Carpaneto, S. Micera, T. Proietti
The Biorobotics Institute and Department of Excellence in Robotics & AI
Scuola Superiore Sant'Anna
56127 Pisa, Italy
E-mail: tommaso.proietti@santannapisa.it

G. Caserta, N. Boccardo
Rehab Technologies Lab
Istituto Italiano di Tecnologia
16163 Genova, Italy

The ORCID identification number(s) for the author(s) of this article can be found under https://doi.org/10.1002/aisy.202500262.

© 2025 The Author(s). Advanced Intelligent Systems published by Wiley-VCH GmbH. This is an open access article under the terms of the Creative Commons Attribution License, which permits use, distribution and reproduction in any medium, provided the original work is properly cited.

DOI: 10.1002/aisy.202500262

N. Boccardo
Open University Affiliated Research Centre
Istituto Italiano di Tecnologia (ARC@IIT)
16163 Genova, Italy

E. Gruppioni
Centro Protesi INAIL
National Institute for Insurance against Accidents at Work
Vigorso di Budrio, 40054 Bologna, Italy

S. Micera
Translational NeuroEngineering Laboratory
Neuro-X Institute, School of Engineering
École Polytechnique Fédérale de Lausanne (EPFL)
1015 Lausanne, Switzerland

S. Micera, T. Proietti
Modular Implantable Neuroprostheses (MINE) Laboratory
Università Vita-Salute San Raffaele
20132 Milano, Italy

26404567, 0, Downloaded from https://advanced.onlinelibrary.wiley.com/doi/10.1002/aisy.202500262 by CochraneItalia, Wiley Online Library on [18/06/2025]. See the Terms and Conditions (https://onlinelibrary.wiley.com/terms-and-conditions) on Wiley Online Library for rules of use; OA articles are governed by the applicable Creative Commons License

Most common approaches focus on vibrotactile feedback,[14,20–23] which is simple, inexpensive, and compact.[10] However, its working principle is based on sensory substitution, which contrasts with the common consensus that the most intuitive and natural way of providing sensory feedback is through biomimicry and bioinspired approaches.[6,24,25] Additionally, vibrotactile feedback can disrupt user concentration,[14] and its long-term effects can be detrimental to fast-adapting mechanoreceptors,[24] raising concerns about its suitability for prolonged use. Tactors, i.e., mechanical devices applying a deformation to the skin through motors, are a potential complementary solution to the vibrotactile feedback approach.[26] However, they are inherently limited by their nonnegligible size, limited adaptability, and lack of comfort.

To address these limitations, soft tactile actuators—highly compliant interfaces that enable safe and gentle interaction with human bodies—have been increasingly investigated for their ability to convert various forms of energy input into mechanical deformation of the skin. Such energy inputs may include electrical (e.g., electroactive polymers such as dielectric elastomer actuators (DEAs),[27] or piezoelectrical actuators)[28] thermal (e.g., shape memory materials),[14] magnetic (e.g., magneto-responsive actuators),[8] or fluidic (e.g., hydraulic or pneumatic systems)[19] sources.

These technologies offer lightweight, flexible solutions with fast response times and the ability to deliver pressure and vibration stimuli. However, they are still limited.[29] Electrical actuators are sensitive to environmental conditions (dehydration of liquids), have a limited force output (mV range), and require high operating voltages (kV range) which can be considered one of their major drawbacks.[28] Furthermore, their fabrication is non-trivial and the result is fragile when scaled up or integrated with deformable substrates.[30] Thermal actuators suffer from slow response times, limited durability, and missing reverse actuation. Magnetic actuators require additional compliant structures resulting in mechanical stress at the soft-rigid interface, high currents to overcome the limited actuation range, and potential heating issues.

Recent efforts have explored the design of soft pneumatic actuators (SPAs) using compliant materials, aiming at overcoming these limitations. In particular, air chambers made from heat-sealable fabric,[31] and polymers[32] have shown significant promise. These actuators are fast and simple to manufacture, extremely thin, yet capable of generating multimodal feedback. Previous studies[13,31,33,34] have primarily explored the use of elastic materials such as silicone and nylon, which, while feasible, exhibit limited performance due to their reliance on high-pressure and the need of being perfectly in contact with the skin to produce meaningful forces. In contrast, the use of hyperelastic materials such as thermoplastic polyurethane (TPU) remains largely unexplored in this context, despite offering potential advantages in mechanical performance, durability and ease of fabrication.

Here, we present the design and validation of a lightweight and ultrathin TPU-based soft SPA (see **Figure 1**A,B) capable of producing a rich range of bioinspired, multimodal tactile stimuli, including both pressure and vibration, surpassing the performance of previous soft actuators reported in the literature (see Figure 1D and Table S1, Supporting Information). The current work focuses on evaluating the actuator on the forearm for prosthetic applications, where sensory restoration is especially critical, as well as on the fingertip—a more sensitive stimulation location relevant to potential future applications such as virtual reality, surgical robotics, and teleoperation.

Our approach offers a simple, highly customizable, and cost-effective manufacturing process that requires less than 10 min. This enables rapid prototyping and easy adaptation for applications in sensory restoration and augmentation, where customization is essential (see Figure 1C). The actuator delivers both high forces—50% greater than prior solutions under similar conditions—and vibration frequencies, doubling the frequency achieved by most existing designs. Despite this high performance, the actuator maintains a remarkably compact form factor, offering a 10–95% reduction in thickness and a 30–80% reduction in weight compared to the current state of the art. Moreover, the actuator can still stimulate the skin when the mounting contact is not perfect, i.e., some distance between the skin and the surface of the actuator is present. This combination of performance, compactness, and adaptability marks a significant advancement over existing solutions, showing potential for integration into most available wearable robotics to enhance sensory feedback capabilities. To demonstrate the performance of the feedback actuator, we conducted a full haptic characterization that includes the pneumatic and mechanical properties, as well as a user-centered evaluation. The user study involved 14 able-bodied participants and three transradial amputees, testing the actuator on three body locations (the fingertip, forearm and residual limb).

2. Results

2.1. Soft Actuators Design and Characterization

The soft actuator, which serves as the interface to the skin, is fabricated using two ultrathin 0.2 mm heat-sealable TPU membranes; see Figure 1A (FT1029, Novotex, Italy). Details of the manufacturing process can be found in the Experimental Section. To evaluate its performance, we manufactured a state-of-the-art actuator, similar to,[34] using TPU-coated nylon (0.3 mm thickness, Ariatex, DD Global Store srl, Italy) of the same size (25 mm diameter) for comparison and measured both actuators' characteristics (see **Figure 2**B). We performed all our recordings up to a maximum supply pressure of 60 kPa; higher pressure led to rupture within the TPU membrane.

The results in Figure 2A indicate that the prototypes achieved equal performance at 60 kPa transmitting forces of 28 N (nylon: 28.1 ± 0.04 N, TPU: 28.0 ± 0.06 N; average $\pm$ standard deviation) when a preload of 1.5 N was applied assuring a perfect surface contact condition. We further investigated the performance by introducing a gap, accounting for variability among human users, such as differences in comfort during the tightening of wearable solutions, which influence the mounting on the body. By increasing the distance between the actuator and the force sensor (gap), distinct differences between the two designs became apparent. As shown in Figure 2A, the TPU design generated 14% more isometric force compared to the nylon-based solution, when a very small gap of 2 mm was introduced

© 2025 The Author(s). Advanced Intelligent Systems published by Wiley-VCH GmbH

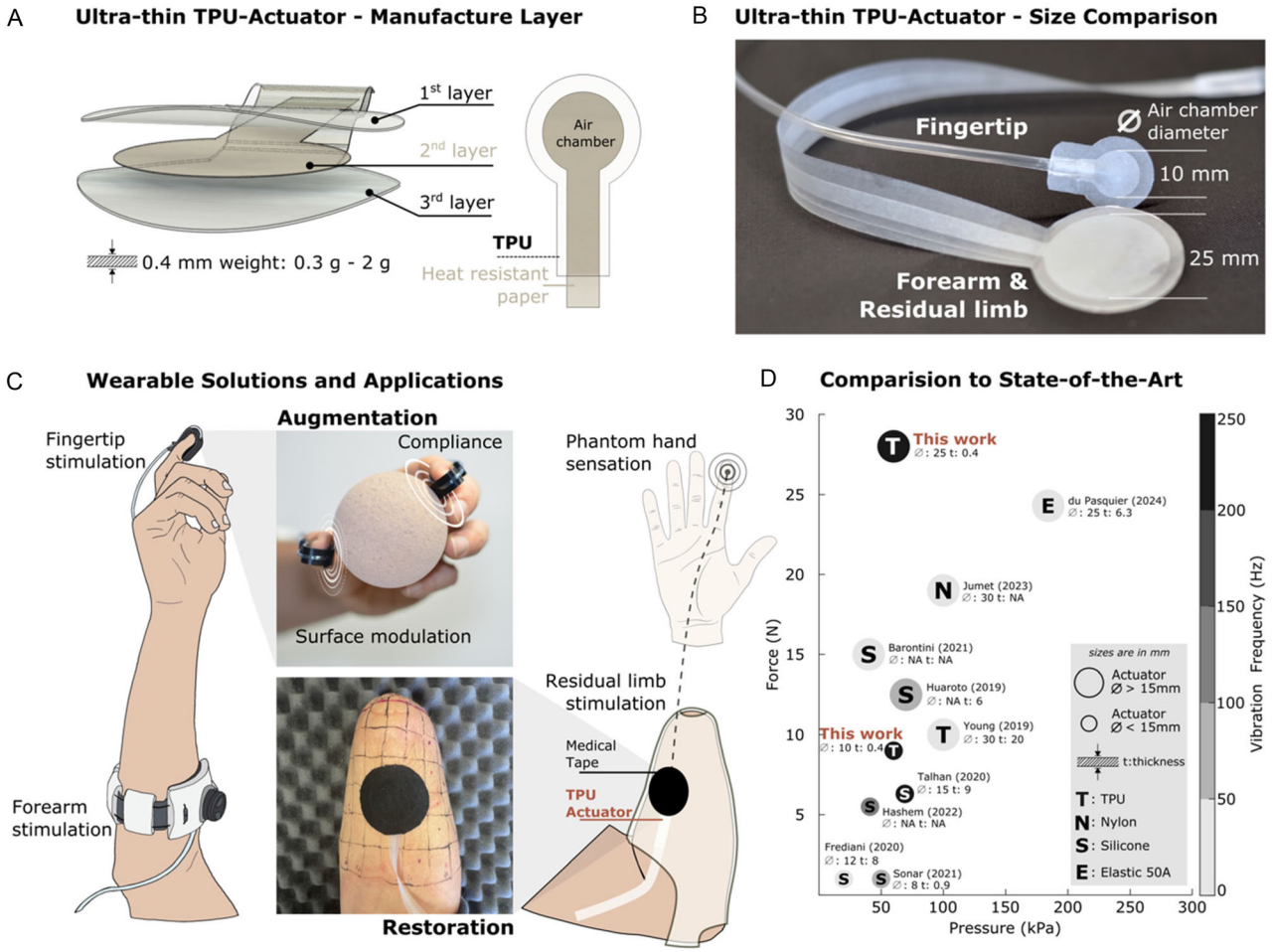

Figure 1. Overview of the ultrathin, lightweight, and multi-modal (pressure and vibration stimuli) soft feedback actuator. A) The actuator is manufactured of TPU. Using heat-resistant paper, the air chamber is created by heat sealing the two TPU layers. An opening towards one side of the actuator allows the insertion of the tube. The resulting 25 mm actuator weighs less than 2 g (without the tube) with a thickness of only 0.4 mm. B) Actuators of different sizes (10 and 25 mm) were produced and tested on humans. The long inlet tube, shown for the 25 mm actuator, allowed comfortable mounting under the socket of a prosthesis. C) Different mounting solutions for the actuator, including fingertip, forearm and residual limb fixations. The fingertip is used for the 10 mm actuator while the forearm and residual limb stimulation used the 25 mm actuators. D) Comparison of the TPU actuator performance to state-of-the-art soft SPAs (only similar technologies were included in the comparison). See Table S1, Supporting Information. Our TPU-based actuator excels in the two existing size categories, reaching higher forces at lower pressure and high vibration frequency.

(nylon: 17.2 ± 0.06 N, TPU: 20.1 ± 0.03 N; average $\pm$ standard deviation). This trend becomes even stronger at 4 mm distance, where the TPU solution generates ≈50% higher forces (nylon: 6.1 ± 0.10 N, TPU: 12.8 ± 0.08 N; average $\pm$ standard deviation). Above 6 mm distance, the nylon actuator was not able to transmit any force, while the TPU still transmitted up to 6.4 ± 0.20 N, showing the clear benefit of the hyperelastic nature of TPU (see Figure S4, Supporting Information).

Four different designs of TPU actuators (10 mm—suitable for average fingertip dimensions—to 25 mm, designed for other body locations) were further evaluated to explore suitability for different applications. As shown in Figure 2C, even the smallest actuator demonstrated the ability to produce meaningful forces, reaching 8.9 ± 0.1 N at 60 kPa (average $\pm$ standard deviation). To ensure the stability and robustness of our actuator, we conducted an endurance test over 1000 inflation–deflation cycles to 30 kPa. The results ensure consistent performance with a maximum variance of 0.1 N and no membrane deformation within the test duration of 100 min (see Figure 2E).

From a thermal stability point of view, the TPU actuator is designed for direct skin contact—within a glove, armband, or prosthetic socket—which provides a stable environment (32–35 °C skin temperature). Nonetheless, we evaluated the material behavior at the high temperatures (150–160 °C) faced during the manufacturing process and found that the heated TPU samples exhibited reduced stiffness and stress levels, indicating a softer, more compliant response to stretch (see Figure S1, Supporting Information for further details).

Humidity may also affect the performance of the actuator, especially considering human sweat and prolonged-term usage. While thorough evaluation of this phenomenon is required, in this study, a single actuator sample was used across all the pilot

© 2025 The Author(s). Advanced Intelligent Systems published by Wiley-VCH GmbH

26404567, 0, Downloaded from https://advanced.onlinelibrary.wiley.com/doi/10.1002/aisy.202500262 by CochraneItalia, Wiley Online Library on [18/06/2025]. See the Terms and Conditions (https://onlinelibrary.wiley.com/terms-and-conditions) on Wiley Online Library for rules of use; OA articles are governed by the applicable Creative Commons License

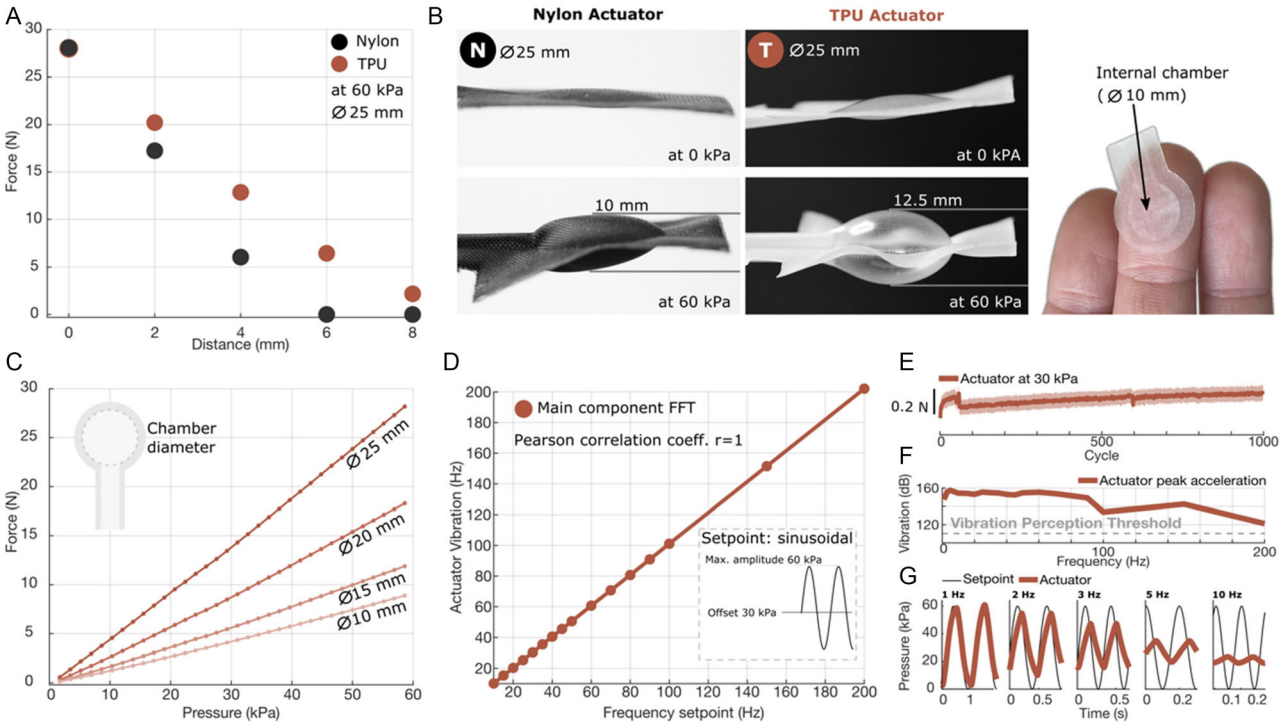

Figure 2. Mechanical characterization of the soft actuator. A) Maximum transmitted force at inflations of 60 kPa for nylon (black) and TPU (red) actuators (mean over three repetitions). With increasing gap (2–8 mm), distinct differences between the two designs are apparent. At 6 mm, the nylon-based actuator is not able to transmit any force on the load cell surface. B) Free-inflation height of the nylon and TPU actuators at 60 kPa. The TPU actuator reached a maximum free inflation of 12.5 mm, the nylon-based solution only reaches 10 mm. C) Isometric force transmission for four TPU actuator with different sizes (10, 15, 20, 25 mm, mean over 5 repetitions, 2 actuators for each size). While decreasing, in the smallest design the actuator was able to produce 8.9 ± 0.1 N at 60 kPa. D) Vibration bandwidth: the main FFT component is linearly correlated to the setpoint frequency (Pearson correlation coefficient of 1). E) Endurance test over 100 min with 1000 inflation/deflation cycles to 30 kPa shows a stable behavior of the actuator with a maximum standard deviation of 0.1 N from the setpoint. F) Vibration acceleration reached during different frequency setpoints (1–200 Hz), always above the VPT,[35] meaning that the stimulation is perceivable by humans. G) Examples of actuator dynamical behavior for sinusoidal setpoints up to 10 Hz.

tests and the experiments with 14 able-bodied participants, for a total of more than 7 h of wear time and approximately ≈3800 inflation cycles across the systems full pressure range (0–60 kPa). During these trials, repeated mounting and donning introduced additional mechanical stress. However, force output of the newly manufactured actuator did not degrade after this extended use (see Figure S2, Supporting Information).

Regarding vibrotactile stimulation, the frequency response of the system was characterized by analyzing acceleration data recorded from an inertial sensor (IMU) placed on the actuator TPU membrane (see Figure S5, Supporting Information). Fast Fourier transform (FFT) analysis revealed a linear correlation (Pearson correlation coefficient = 1) between the setpoint frequency (1–200 Hz) and the measured signal (see Figure 2D). The additional frequency components that can be found (see Figure S6, Supporting Information) can be likely explained by the coupling between the TPU membrane and the IMU, thus affecting the acceleration. Additionally, the maximum acceleration values remained above 120 dB (see Figure 2F), despite the non-negligible weight of the IMU (30 g), exceeding the vibration perception threshold (VPT) for the human index finger in able-bodied individuals under the age of 60 (VPT:115.2 dB up to 250 Hz,).[35] These results confirm the system's ability to generate effective vibrotactile feedback.

2.1.1. Air Supply System

For any pneumatic system, the stability, repeatability, and dynamic performance depend on the air supply system. In this work, the inflation was controlled by using a prototype portable control unit (Figure S7 and S8B, Supporting Information), including a pump (SPV35RO-12FC-A-DV, Schwarzer Precision GmbH, Germany) and a custom soft air accumulator, manufactured following the same procedure as the soft actuator but in a bigger size (12 cm × 7 cm, fitting ≈160 mL at 70 kPa). The accumulator is used to reduce the activations of the pump thus limiting noise which is a common drawback of pneumatic systems. The pneumatic circuit was regulated by two normally closed proportional valves (VSO MAX HP model 2, Parker Corporation, USA) mounted on a 3D-printed custom manifold (Grey-Pro Resin, Foarmlabs, USA). Two pressure sensors (one for the actuator, one for the accumulator) closed the control loop (ABPDANV060, Honeywell International, USA) together with a microcontroller (Feather M4 Express, Adafruit Industries, USA) running a proportional–integral–derivative (PID) pressure control loop at 500 Hz. The lightweight control box weighs 585 g, including a 125 g power supply and a 150 g pump, and measures 14 cm × 16 cm × 8 cm. Notably, the overall size and weight are comparable to other wearable technology for prosthesis

© 2025 The Author(s). Advanced Intelligent Systems published by Wiley-VCH GmbH

26404567, 0, Downloaded from https://advanced.onlinelibrary.wiley.com/doi/10.1002/aisy.202500262 by CochraneItalia, Wiley Online Library on [18/06/2025]. See the Terms and Conditions (https://onlinelibrary.wiley.com/terms-and-conditions) on Wiley Online Library for rules of use; OA articles are governed by the applicable Creative Commons License

users in literature (e.g., ref. [16]). Considering weight, margin to improve lays in replacing the power supply with thin Li–Po batteries which would also make the system untethered. At the same time, the pump could be replaced by a CO_2 canister, which would also dramatically reduce noise and size in exchange of a shorter lifetime before substitution with a new canister (e.g., what was proposed by ref. [36] in a similar pneumatic system). Regarding noise, due to appropriate isolation of the control box including a silencer on the pump air intake, the running system produces only 52.0 dB of noise, with a peak of 57.5 dB when the pump is filling the reservoir. For reference, this is comparable to the noise level of an office or a normal conversation.[37] Measurements were recorded using a Sound Level Meter (72-942, Multicomp Pro, USA) in a background noise environment of 42 dB.

Additionally, the number of air chambers can be increased to create an actuator array, though independent activation comes at the cost of adding valve to the pneumatic control box (see Figure S7, Supporting Information). Pressure levels and waveforms were set through a custom graphical user interface, while participant answers were gained over a touchpad.

2.2. User Study

To validate the versatility and simplicity of use of our actuator, we conducted a user study comprising three distinct experiments. In the first experiment, we assessed the just noticeable difference (JND) among a group of 14 able-bodied participants (4 women, 10 men; mean age 26 ± 2.4 years) and three male individuals with transradial amputations (mean age 51.3 ± 13.6 years). The second experiment involved five able-bodied participants who performed a perception-matching test, exploring three different surface textures to evaluate the system's ability to convey nuanced tactile information. Finally, the third experiment focused on the three participants with amputations, testing their accuracy in characterizing levels of force intensity and the type of elicited sensations delivered by the feedback system. For able-bodied, the quality of the elicited sensations was rated in a final questionnaire (for the full questionnaire, see Table S2, Supporting Information).

The test on able-bodied was performed on the forearm mounting the 25 mm actuator and, on the fingertip, mounting the 10 mm actuator. The test on amputees, instead, was performed using the 25 mm actuator on one remapping spot on the residual limb, producing unique sensations on the phantom hand. The full procedure to locate the remapping spots and mount the actuator is described in the Section 4.

Each participant provided written informed consent prior to the study, which followed the principles of the Declaration of Helsinki and received approval from the Territorial Ethics Committee of the Liguria Region (Protocol code: IIT_REHAB_HT01) and by the Joint Ethics Committee of the Scuola Normale Superiore and the Scuola Superiore Sant'Anna (Protocol code: 18/2023).

2.2.1. Just Noticeable Difference Threshold

Participants performed a two-alternative forced choice (2AFC) test, in which they were presented with pairs of stimuli (10, 22.5, 35, 47.5, and 60 kPa, always compared to 35 kPa) and repeatedly asked to determine which stimulus in each pair felt stronger. **Figure 3**A illustrates the JND results for the three tested conditions. For able-bodied participants, the mean JND for the forearm was 7.0 ± 0.22 kPa, and for the fingertip, it was 6.5 ± 0.23 kPa. In the amputee group, the mean JND was slightly higher, with 7.7 ± 1.1 kPa (mean values $\pm$ standard error).

The Weber fraction k, defined as the ratio of the JND to the RS intensity, was calculated. This fraction quantifies how much a stimulus must change for a person to detect a difference. The calculated values were 20%, 19%, and 22% for the forearm, fingertip, and remapping spot on the residual limb, respectively (higher values indicate lower sensitivity).

In Figure 3A, the individual responses of the able-bodied (forearm) and amputee participant are shown along with the fitted sigmoid curve. This curve was used to calculate the individual JND, as described in the Section 4. The x-axis represents stimulus intensity, while the y-axis (ranging from 0 to 1) indicates the proportion of CS perceived as stronger than the RS, i.e., CS > RS. All individual able-bodied results from the 2AFC test are provided in Figure S9, Supporting Information.

The scoring (range 1–7) of the questionnaire able-bodied participants filled after the test is shown in Figure 3C. The overall scoring of the participants with small variation is indicating a clear consensus regarding the comfort, pleasantness, pain, and willingness to longtime use of the fingertip and forearm interfaces (full questionnaire in Table S2, Supporting Information).

2.2.2. Perception-Matching Test

Five able-bodied participants compared three virtual stimuli presented simultaneously against a real surface—grating with 1 mm spacing, grating with 4 mm spacing, and a smooth surface. Participants rated how similar the virtual stimuli felt compared to the real surfaces. The results of the perception-matching test showed ratings for smooth, 1, and 4 mm surfaces of 0.6 ± 0.1, 0.7 ± 0.1, and 0.6 ± 0.3 in the case that the virtual stimuli were designed to match the real surfaces ("fully matching" defined as 1.0, average $\pm$ standard deviation). For the different stimuli, the ratings were 0.1 ± 0.1, 0.2 ± 0.1, and 0.2 ± 0.1, for smooth, 1, and 4 mm surfaces (average $\pm$ standard deviation). The results are shown in Figure 3B, with the similarity rating on the y-axis (ranging from "not at all" to "fully matching") and the type of virtual stimulus on the x-axis. The label "same" indicates that the virtual stimulus was designed to match the real surface, while the other label "diff" represents the ratings for the two additional virtual stimuli that were different from the real surface.

The scoring (range 1–7) of the questionnaire participants filled after the test is shown in Figure 3C. The pleasantness (6.0 ± 1.1) and naturalness (6.6 ± 0.5) of the stimuli were rated very high. Given the small group size ($n = 5$), no statistical analysis was carried out to compare the vibration–pleasantness scoring against the pressure–pleasantness (JND-task).

2.2.3. Intensity Characterizations Test

Three amputees participated in a classification task in which they categorized 60 stimuli into three intensity levels: low,

© 2025 The Author(s). Advanced Intelligent Systems published by Wiley-VCH GmbH

26404567, 0, Downloaded from https://advanced.onlinelibrary.wiley.com/doi/10.1002/aisy.202500262 by CochraneItalia, Wiley Online Library on [18/06/2025]. See the Terms and Conditions (https://onlinelibrary.wiley.com/terms-and-conditions) on Wiley Online Library for rules of use; OA articles are governed by the applicable Creative Commons License

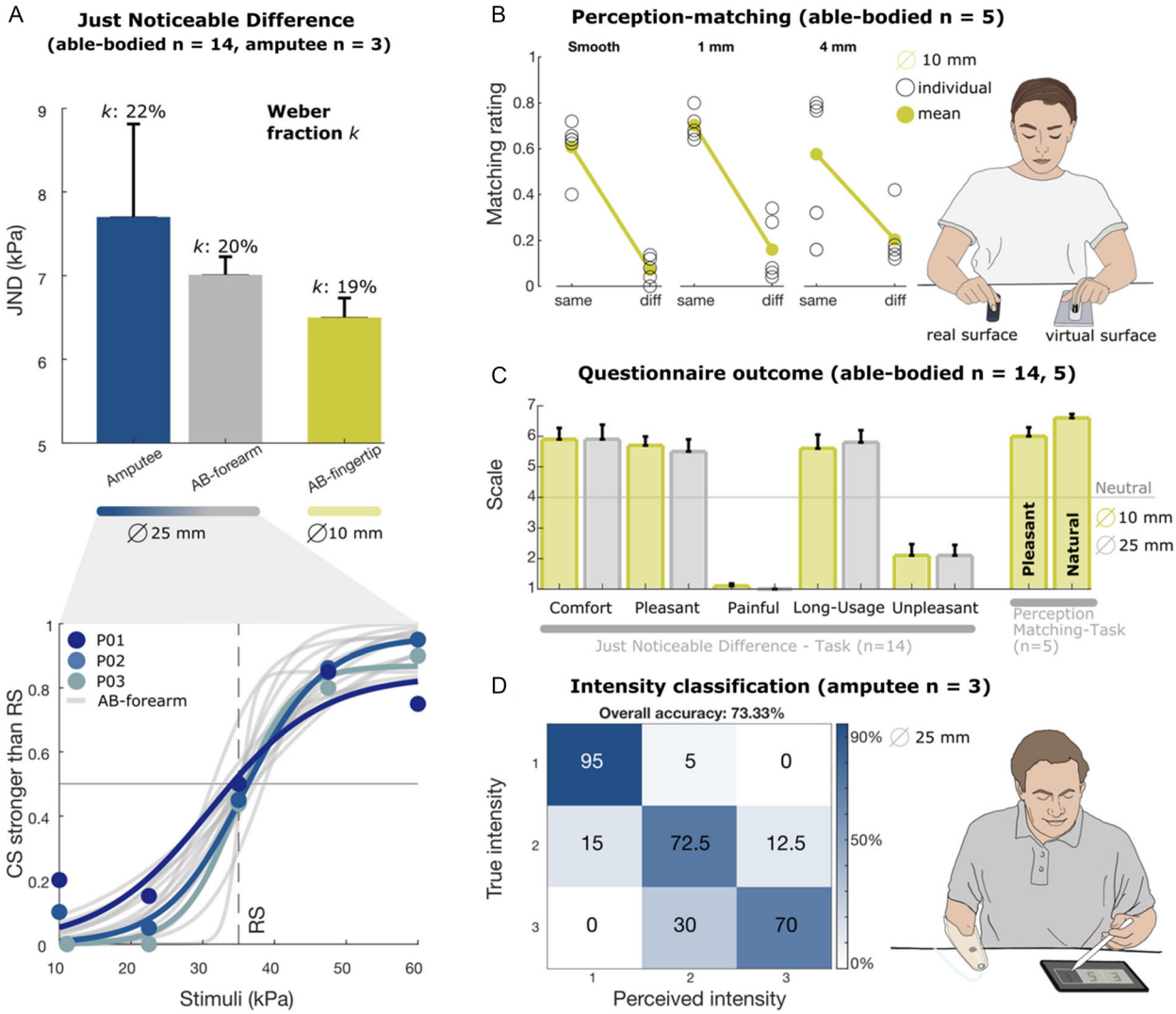

Figure 3. Overview of the results of the user study. A) Comparison of the mean JND results for the three tested conditions as a bar plot (mean values ± standard error) with the corresponding Weber fraction *k*. AB: able-bodied. The mean for the amputee group was slightly higher (7.7 ± 1.1 kPa) compared to the able-bodied (forearm, 7.0 ± 0.22 kPa). The lowest JND values were found for the fingertip condition (6.5 ± 0.23 kPa). On the bottom, the individual performance of each participant (able-bodied in grey, amputees in blue). The circles show the data for the summed response for each of the five stimuli levels, where the comparison stimuli (CS) were judged stronger than the reference stimulus (RS), within 20 repetitions. The RS at 35 kPa is shown by the dashed vertical line. In case of comparison between equal stimuli (CS = RS), participants were expected to score close to 0.5 (indicated by the solid horizontal line). The lines show the sigmoid fit to the summed response. A difference in the slope of the sigmoid corresponds to higher or lower JND values (computed as the mean between the point of subjective equality—PSE, 0.5 on the fitted psychometric function—and the intensity values at the 0.25 and 0.75 points on the psychometric function). B) Perception-matching outcome, with the able-bodied participants asked to compare real and virtual surfaces. The individual mean data (black circle) is plotted together with the overall group rating (yellow circle). The label "same" indicates that the virtual stimulus was designed to match the real surface, while the label "diff" represents the ratings for the two additional virtual stimuli that were different from the real surface. C) Overview of the questionnaire (full questions can be found in Table S2, Supporting Information) highlighting the positive feedback from the participants regarding the stimulation and wearable comfort as well as the high naturalness perceived. The mean rating and standard error are shown. Questions concerning the JND were answered by all able-bodied participants (n=14), while the last two questions (naturalness and pleasantness) were only answered by the subgroup conducting the perception-matching task ($n = 5$). D) Intensity classification results show the overall performance of the three amputees, with an accuracy of 73.3%. The lowest intensity level was selected with 95% accuracy, while the middle and highest intensity included more false decisions, indicating that participants perceived it difficult to separate these levels (but still largely above the chance level, 33%).

medium, and high. The overall classification accuracy was 73.3%, higher than the chance level of 33.3% for random guessing. For details on individual accuracy, see Figure S10, Supporting Information.

Despite the differences in individual phantom hand sensations stated in the mapping process (shown in **Figure 4**A), on average, the sensations elicited during the test by the actuator across the three amputees were dominantly Pressure (25%)

© 2025 The Author(s). Advanced Intelligent Systems published by Wiley-VCH GmbH

26404567, 0, Downloaded from https://advanced.onlinelibrary.wiley.com/doi/10.1002/aisy.202500262 by CochraneItalia, Wiley Online Library on [18/06/2025]. See the Terms and Conditions (https://onlinelibrary.wiley.com/terms-and-conditions) on Wiley Online Library for rules of use; OA articles are governed by the applicable Creative Commons License

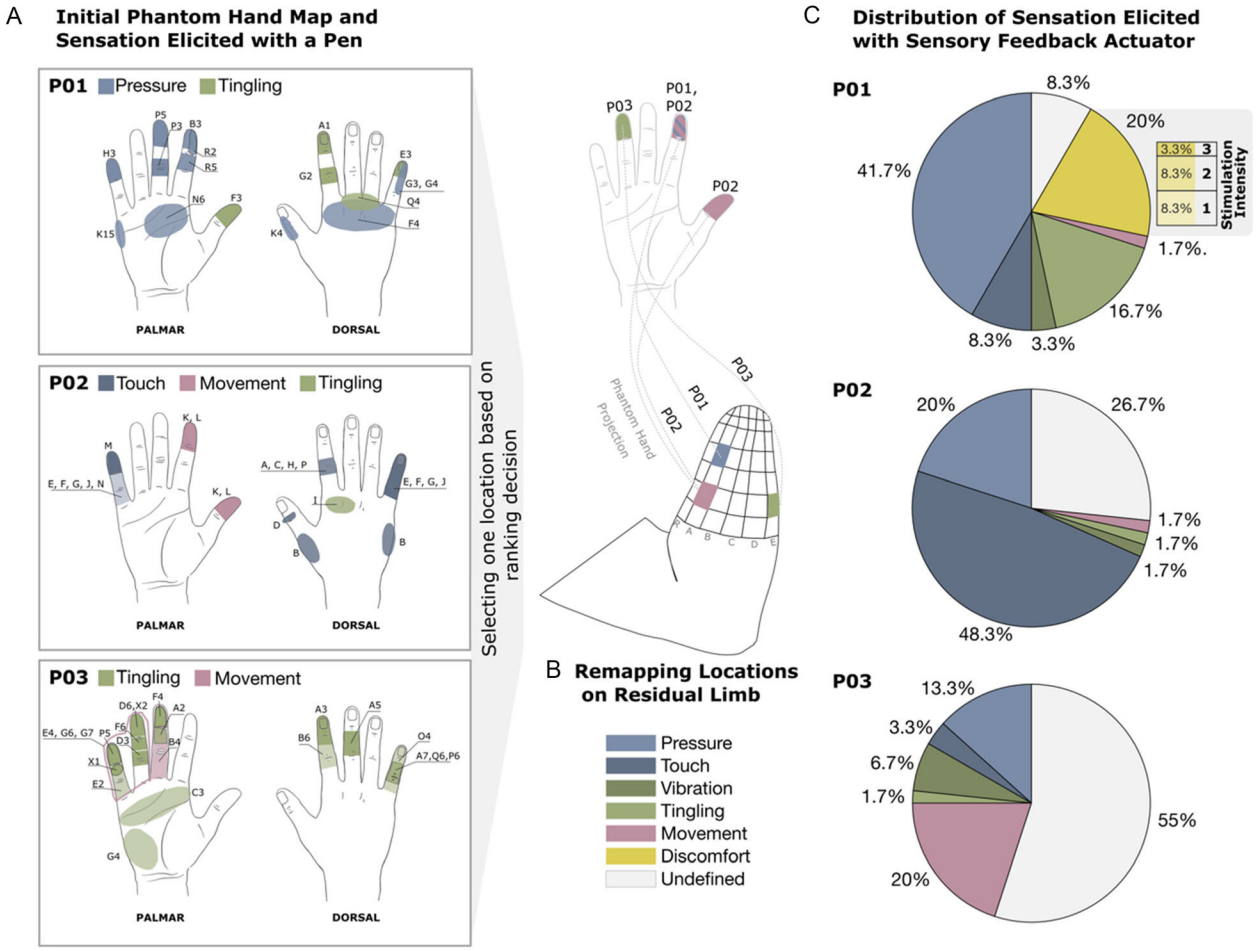

Figure 4. Overview of the elicited sensations during the study involving amputees. A) The initial mapping locations and types of sensations elicited with the round end of a pen. Across the three amputees, the sensations ranged from pure pressure/touch sensations to movement and tingling perceptions in the phantom hand. The letters label the phantom sensation map and correspond to unique locations on the residual limb. B) The single locations on the residual limb used during the user study and their corresponding projected phantom sensations and locations. The specific locations were selected based on a ranking that prioritized palmar fingertip locations due to their importance in daily interactions with the prosthetic hand. For participant P02, stimulation activated two phantom hand locations—namely, the index and thumb fingertips—creating a sensation as if the fingertips were moving toward each other in an "OK" sign. C) Distribution of the sensations elicited when the actuator stimulated the residual limb during the classification task at three intensities (60 stimuli in total). Participants labeled their sensations using the terms "Pressure," "Touch," "Vibration," "Tingling," "Movement," "Discomfort," and "Undefined" based on ref. [38]. "Undefined" was selected when no label matched their sensation. The indication of "Movement" may, in addition to the phantom sensation, be linked to the actuator's physical activation (inflation/deflation). Discomfort in P01 occurred at all stimulation levels. As it was already present at the lowest stimulation level (8.3%), it was likely the results of other external factors affecting comfort (e.g., sweating, task duration).

and Touch (20%), while Movement (7.8%), Tingling (6.7%), Discomfort (6.7%), and Vibration (3.8%) were reported less frequently (see Figure S11, Supporting Information). A high proportion of Undefined (30%) suggests that the provided labels (following ref. [38]) did not fully capture all sensations experienced. The indication of Movement (7.8%), apart from being present at the residual limb, may partially be attributed to the actuator's physical activation, which could have been perceived as movement (inflation/deflation).

Individual distribution of elicited sensations is shown in Figure 4B,C. It is interesting to highlight the shift in the dominant sensation of the initial phantom spot for P02 and P03. For P02, the sensations shifted from the initial Movement sensation to Touch/Pressure (68%). For P03, the sensations changed from only Tingling to more versatile ones, including 16% Touch/Pressure and 20% Movement, leaving only 8% to Vibration/Tingling. If we do not consider undefined sensations, the initial sensation of P01 for the selected remapping location, namely Pressure, stayed instead dominantly (49% Touch/Pressure).

P01 was also the only participant reporting Discomfort (20% of cases). However, the fact that discomfort was perceived at the lowest stimulation level (8.3%) suggests that it may have been influenced by external factors to the stimulation, such as socket fit, task duration, or sweating—none of which were investigated in this study.

© 2025 The Author(s). Advanced Intelligent Systems published by Wiley-VCH GmbH

26404567, 0, Downloaded from https://advanced.onlinelibrary.wiley.com/doi/10.1002/aisy.202500262 by CochraneItalia, Wiley Online Library on [18/06/2025]. See the Terms and Conditions (https://onlinelibrary.wiley.com/terms-and-conditions) on Wiley Online Library for rules of use; OA articles are governed by the applicable Creative Commons License

3. Discussion

Haptic interfaces have the potential to significantly improve the overall user performance by providing rich sensory information in many robotic devices (e.g., artificial limbs) and applications such as virtual reality and teleoperation. However, current solutions face several challenges, including requiring high pressure to provide meaningful forces that are significantly impacted by suboptimal wearing (e.g., gap between skin and actuator), thick designs that reduce the possibility to be integrated in current robotic systems, lack of multimodal feedback, and, considering prosthetics, lack of validation in amputees. In this article, we explore a TPU-based design for an ultrathin, lightweight, soft actuator for multimodal tactile sensory feedback, whose performance goes beyond conventional silicone-based as well as HST-based actuators. Moreover, this work represents the first in-depth validation of a soft feedback TPU actuator on both able-bodied individuals and amputees, including both a psychometric and a functional characterization.

Our compact inflatable actuator is manufactured using a cost-effective, quick 10-min process (as a reference, the common Dragon Skin silicones have a cure time ranging from a minimum of 30 min up to a few hours), allowing a high degree of fast customization. Compared to state-of-the-art silicone-based solutions, our biggest actuator (diameter 25 mm) demonstrates weight (at least 30% below previous work,[19] despite our actuator being twice the diameter) and thickness reductions (at least 10% below previous work[32]). Even when compared to previous HST-based solution,[31] we were able to observe reduction in weight (80%) and thickness (96%) despite the same chamber dimension. Improved form factor, in terms of both lower weight and thickness, is crucial for integrating the actuator into current robotic platforms, such as artificial limbs, without requiring complex modifications. The actuator interface itself, with a thickness of only 0.4 mm, can be easily incorporated as a proof of concept into many wearable systems. This allows for quick evaluation of important parameters such as size and placement and whether haptic feedback would be beneficial, before proceeding with proper integration which would require mechanical modifications to the system (including a non-negligible integration of a compressed air source).

However, a thinner actuator could be weak in terms of transmitted force, robustness, and durability. We demonstrated that despite a lower inflating pressure (60 kPa), our 25 mm design provides an improvement of 47% in force output with respect to existing solutions under similar conditions (HST-based, 30×30 mm, 100 kPa[34]). The robustness of our solution was validated with an endurance test including over 100 min of continuous cycles of inflation/deflation resulting in minimal variation of force (0.1 N). Moreover, the system reaches up to 200 Hz, with a minimum of 120 dB vibration, which is more than double of most solutions in literature, and second only to Talhan et al. (250 Hz[39]).

We assessed the functionality of our feedback system in three distinct experiments. These experiments demonstrate the systems applicability across diverse user groups in augmentation and restoration -tasks, highlighting its potential for broader implementation. The results of the standardized psychometric tests allow comparison across different populations, including those with sensory impairments. The measured k, 19% fingertip and 20% forearm in able-bodied, and 22% in amputee, are within values for force discrimination found in literature on soft feedback actuators (Frediani et al.[19] Barontini et al.[40]) where higher values indicate a lower sensitivity. However, in both cases, their systems produce lower forces (1 N at 20 kPa for Frediani and 15 N at 40 kPa for Barontini) when compared to ours (28 N at 60 kPa), which still translate into a more versatile and powerful feedback capability for our solution. Importantly, high forces at lower pressure directly and positively impact the air supply system, easily the largest component affecting wearability and portability.

We conducted perception-matching tests with a subgroup of 5 able-bodied participants and demonstrated the practical capability of the actuator in conveying the tactile characteristics of virtual surfaces, particularly at different levels of roughness to the fingertip. While previous works have included other functional assessments (e.g., pattern and texture recognition,[41] mirror box experiment of sensation mapping,[42] and directional cues classification[34]), the lack of standardized tests, and thus uniform metrics, and the absence of psychometric characterization, make a direct comparison challenging.

In a discrimination test with three amputees, we observed high accuracy above chance (73.3%) when classifying stimuli of different intensities. These results are comparable to the outcome of Valle et al. ,[43] using invasive biomimetic intraneural electrical stimulation, reaching an accuracy of 70%. For the non-invasive case, soft pneumatic solutions have rarely been tested on amputee for three levels (i.e., Antfolk et al.[44] two levels, finding 90% accuracy with a chance level of 50% on PHM spots on amputee and 80% in able-bodied; Simons et al.[14] three levels, soft nonpneumatic, 20 able-bodied participants only 66% accuracy). Following up on this application, future work will address the full integration of the sensory feedback system, including closed-loop control of a prosthetic hand, to conduct further tests such as object size and compliance discrimination, which can be found more frequently in literature.

Restoring or augmenting sensory feedback has the goal of making the experience as natural and intuitive as possible while creating a realistic touch illusion. Therefore, the quality of sensation plays a key role in how users accept and integrate a haptic device into their experience. In this study, able-bodied participants rated the comfort and pleasantness of stimulation delivered by the actuator as very high (5.9 and 5.7 out of 7). Additionally, when rendering surfaces at a high dynamic range, participants further confirmed a natural sensation (6.6 out of 7). While sensory feedback restoration in amputees has been widely tested using both noninvasive and invasive methods, the resulting quality and range of sensations differ significantly from those of able-bodied individuals. This difference arises due to the cause of amputation, the surgical procedure, which can alter nerve sensitivity and organization. Additionally, the way sensory information is transmitted to the afferent nerves plays a crucial role in the elicited sensations—either mechanically through the skin, with or without relying on the phantom phenomenon, or directly via electrical stimulation using invasive interfaces. Although the range of sensations in our approach could be limited to the initial phantom hand map, we observed a notable shift towards pure touch sensations. The high percentage of pressure and touch

© 2025 The Author(s). Advanced Intelligent Systems published by Wiley-VCH GmbH

26404567, 0, Downloaded from https://advanced.onlinelibrary.wiley.com/doi/10.1002/aisy.202500262 by CochraneItalia, Wiley Online Library on [18/06/2025]. See the Terms and Conditions (https://onlinelibrary.wiley.com/terms-and-conditions) on Wiley Online Library for rules of use; OA articles are governed by the applicable Creative Commons License

reported (45%, combined) highlights the potential of the ultrathin actuator for impaired populations. We furthermore found no touch sensations in P03 in the initial mapping, whereas they were elicited with the actuator stimulation (16%). Additionally, participants reported a perceptual shift when comparing the initial mapping done with a pen to the sensations elicited by the actuator.

Qualitative feedback also conveys the promise of the proposed technology. P02: "The sensation with the actuator is very different compared to the pen; it feels less on the surface of the skin and more on the phantom hand." P03: "Most phantom hand locations initially felt like tingling and paresthesia, extending to the finger. However, with the actuator, the tingling sensation disappeared, leaving mostly touch." These statements resulting from our preliminary study show the potential for sensation shift which the actuator in combination with a direct encoding could provide. We further emphasize that this approach can be used for amputees who do not experience phantom sensations, as the direct translation of pressure from the prosthesis hand sensor to the actuator on the skin still provides a straightforward, bioinspired encoding, resulting in modality but not location matching. These two points will need to be investigated in future work, including a more diverse group of participants using a bidirectional prosthesis.

Matching the quality and type of sensations to natural physiological ones in populations with sensory loss remains a challenge in state-of-the-art research.[45] In the noninvasive approach of Gozzi et al.[46] who restored lost foot sensation using transcutaneous electrical nerve stimulation (TENS), a high proportion of vibration/tingling (70%) and electricity (9%), with a low percentage of touch/pressure sensations (6%) was found. Notably, the study did not assess unpleasant sensations. Examples of invasive approaches that elicit phantom hand sensations in amputees, using direct nerve stimulation such as the work by Valle et al.[47] reported that the sensations were perceived as very different from the natural touch. The reported distribution of touch/pressure sensations in two amputees never exceeded 17%. Sensations of electricity/vibration dominated, often activating large areas of the hand. A finer degree of control over the elicited sensations was reported by Tan et al.[48] where two participants described the perceptions as natural, including a wide range of sensations. Despite promising, it is important to underline that invasive solutions come with the significant impact of surgery, associated costs (which are currently not covered by the healthcare system), and the personal decision to undergo an implant. A noninvasive solution like the one presented in this work, which is reaching similar or beyond performances, is more likely to become commercially available and thus impacting a greater group of people.[45]

Importantly, and in contrast to invasive solutions, we showcased the simplicity of the proposed soft actuator that can "stick" to the skin, without any complicated integration processes (e.g., physical modification of the prosthetic socket for amputees). The modality can be switched between touch/pressure and vibration depending on user preferences or application needs. This approach can be applied to any research on human-robot interaction requiring sensory feedback, whether for restoration or augmentation.

While our system demonstrates great advancements in both design and performance, certain limitations must still be acknowledged. From a technical standpoint, the system's sampling frequency (500 Hz) restricted the maximum vibration frequency we could test to 200 Hz. Additional experiments will be carried out to confirm that the feedback system can achieve even higher vibration frequencies.

The user study was limited due to the absence of a true closed-loop system with real-time sensing of surface properties, relying instead on predefined parameters. Integrating sensors to record actual surface characteristics (prosthetic hand) and enhancing the sensory feedback with virtual visual effects could significantly improve the user experience with the system. To minimize variation between users, future designs should include the sensorization of the actuator surface (such as stretch-sensitive sensors) in addition to controlling the internal pressure of the actuator. Our initial testing has stimulated one location at a time, but stimulating multiple locations simultaneously remains a common limitation for noninvasive feedback solutions for amputees, which will be addressed in future work.[49] For long-term applications and integrated solutions, future studies should also investigate potential changes in surface properties, ideally using the aforementioned stretch sensor embedded within the TPU membrane. While we anticipate the actuator itself to be low-cost, long endurance is necessary to increase the potential for user acceptance in real-life wearable systems.

Finally, miniaturization and noise reduction of the pneumatic control unit will be important considerations in future studies, particularly those involving activities of daily living. These aspects were not required in the current study, where participants wore noise-canceling headphones to eliminate environmental distractions and all tests were conducted in a seated, tabletop configuration. Practically, the already low noise generated by our pneumatic system could be mitigated by replacing the pump and reservoir with a compact CO_2 cartridge and pressure regulator, as demonstrated in a fully integrated pneumatic prosthesis socket by Tanriverdi et al.[36] In addition, recent advances in miniaturized pneumatic systems—such as piezoelectric and conventional micropumps, as demonstrated in the FlowIO platform, used for haptic feedback in the HaptiKnit system[50] offer promising directions for reducing the size and weight of pneumatic components, thereby enhancing portability and wearability.

As the applications for haptic feedback continue to grow, our actuator's reduced physical footprint, improved customization, and enhanced performance make it a promising solution for applications where space and weight are critical factors (e.g., artificial limbs). We anticipate from our preliminary user tests that our approach will allow for fast proof of concept, without requiring complex modifications, into existing systems including prostheses, exoskeletons, supernumerary robotics, teleoperation, and virtual reality, without the need for extensive modifications, further underscoring its practical applicability and the importance of the findings.

4. Experimental Section

Objective and Design: The objective of this study was to design and validate a sensory feedback device, encompassing a soft SPA and its

© 2025 The Author(s). Advanced Intelligent Systems published by Wiley-VCH GmbH

26404567, 0, Downloaded from https://advanced.onlinelibrary.wiley.com/doi/10.1002/aisy.202500262 by CochraneItalia, Wiley Online Library on [18/06/2025]. See the Terms and Conditions (https://onlinelibrary.wiley.com/terms-and-conditions) on Wiley Online Library for rules of use; OA articles are governed by the applicable Creative Commons License

controller. The experiments aimed to determine the device's key mechanical characteristics and assess its psychometric and functional performance with able-bodied and individuals with upper limb amputation, as representative of two potential applications (sensory augmentation in virtual reality and restoration in prosthetics).

Actuator Manufacturing Process: The manufacturing process of the soft actuator consisted of a few steps. Importantly, the main features, such as size and shape, can be easily adjusted to fit the body mounting location and the specific application without impacting the duration of the process.

First, the actuator shapes were cut out of TPU and heat-resistant paper using a laser cutter. Then, the layers were manually assembled (see Figure 1A), in the following order: first, the TPU; second, the heat-resistant sheet to prevent the melting of the TPU layers in the air chamber area; third, again, the TPU. Importantly, the heat-resistant separator was also placed towards one extremity of the actuator to allow the insertion of the air tube. A custom aluminum frame was placed between a heat press plate and the assembled layers to protect the TPU chamber area from excessive heat. However, it was also possible to heat seal the actuator without using the custom frame. This approach came at the cost of altering the stretchability of the TPU membrane (see Figure S1, Supporting Information). After the assembly, the actuator was sealed using a heat press (temperature 155°, duration 100 s) taken out, and a weight was applied to it to prevent any warping, which may occur due to rapid cooling. After cooling off, the heat-resistant separator (second layer, Figure 1A) was removed. The soft actuator resulted in being 0.4 mm thick and weighed less than 2 g. Finally, a PVC tube (TUH0604, SMC, USA) was sealed within the inner sides of the TPU channel, using a hot air gun (see Figure S3, Supporting Information) to allow for the actuator inflation. Depending on the actuator air chamber size, tubes with an external diameter of 2 or 4 mm were used. The total manufacture time was less than 10 min.

Mechanical Characterization Tests—Isometric Force Test: The isometric force test measured the relationship between transmitted force and inflation pressure. The recording was performed with a load cell (1 kN max force) within a universal material tester (Instron 5965, Instron Corporation, USA). The soft actuator was placed in a rigid 3D-printed custom mounting, allowing only upward inflation. For the 0 mm distance condition, a preload of 1.5 N was applied. For the increased distance recordings of 2, 4, 6, and 8 mm, the distance measured by the universal material tester position control was used. For the recording, one TPU and one nylon actuator (25 mm in diameter) were used for each design. The actuators were inflated using air pressure levels ranging from 0 to 60 kPa, in 1.7 kPa steps, with three repetitions for each actuator. The control signal comprised a stepped train of square waves with 5-s plateaus at increasing amplitudes and 1-s pauses at 0 kPa between steps (negligible rise time). This protocol was also repeated in the 0 mm distance testing condition, while sweeping the air chamber diameter sizes for the TPU actuator (10, 15, 20, and 25 mm, 5 repetitions, 2 actuators for each size).

A further endurance test in the 0 mm distance test condition was performed using one 25 mm TPU actuator. Measurements were performed over 100 min of continuous inflation/deflation cycles (5 s inflation, 1 s deflation) from 0 to 30 kPa.

Mechanical Characterization Tests—Vibration Test: To analyze the vibration characteristics of the feedback system, 20 different frequencies responses were tested (1, 2, 3, 5, 10, 15, 20, 25, 30, 35, 40, 45, 50, 60, 70, 80, 90, 100, 150, and 200) Hz. The frequencies were selected around the sensitivity of the mechanoreceptors (SAI receptors are associated with primarily static indentations and low-frequency vibrations; RAI receptors are most sensitive at 40–60 Hz ;[51] RAII receptors respond most sensitive to high-frequency vibrations between 100–400 Hz),[51] while the maximum was defined by the updating frequency of the controlling system (500 Hz). For every frequency, a dataset consisting of a 5-s baseline (used for the three-axis accelerometer calibration) and 5 s of vibration was collected. The pressure level setpoint and actuator pressure were recorded by the control system. The setup for the recording consisted of a TPU actuator (25 mm) fixed to a custom rigid 3D-printed mounting allowing inflation only towards the upper direction. A three-axis accelerometer (MPU 6050, TDK *IvenSense* Inc., USA) was used to validate the vibrations following.[39,41] The accelerometer was attached to the top expanding surface and connected to a microcontroller (Arduino Mega 2550, Arduino, Italy), sampling at 800 Hz. The 3D-printed mounting was placed on foam, while the air supply controller was placed on a separate table, to reduce unwanted vibration sources, such as the pump activation. The time and frequency domains were analyzed using MATLAB (R2023b, Mathworks, USA). Raw acceleration data was first recalibrated offsetting the reading such that it read 0 m s^{-2} in the static position and then low pass filtered ($fc = 250$ Hz). The frequency accuracy was analyzed by identifying the main frequency component present in the spectrum (fast Fourier transformation, FFT) and computing the linear correlation of each value with the corresponding setpoint. The peak acceleration (dB) was calculated for each frequency setpoint and compared to the VPT in able-bodied humans presented in ref. [35].

Testing Protocol: User Study—Able-Bodied Participants: Fourteen able-bodied individuals (4 women, 10 men, aged 26 ± 2.4 years, 13 right-handed) participated in a single-session trial. Two stimulation locations were chosen for the experiment: the index fingertip and the inner forearm, both on the nondominant side. The two locations were selected due to their difference in sensitivity and potential applications. The fingertip is highly sensitive because of its high number of mechanoreceptors (slowly adapting afferents 241 units cm^{-2}),[52] making it an ideal location to test the system's precision and responsiveness to fine stimuli. In contrast, the cutaneous skin of the forearm has fewer nerve endings (slowly adapting afferents 6.5 units cm^{-2}),[52] providing a different sensitivity profile that helps evaluate the system's performance across varying levels of tactile sensitivity. In addition to their different mechanoreceptor densities, the two locations were selected as they cover a range of practical applications (e.g., virtual reality, prosthesis).[31] The forearm feedback actuator included a 25 mm-diameter actuator, placed using a one-size-fits-all bracelet (participant circumference at stimulation location: 20–30 cm, with a forearm length range of 21–27 cm) specifically designed for the experiments (Figure 1C). The bracelet was fixated at 25% of the forearm length, measured from the elbow, tightened using a BOA-like fit system ensuring stability for the stimulation and comfort for the participant. The fingertip feedback actuator, including a 10 mm-diameter actuator, was fixed with the custom mounting shown in Figure 1C. Participants could choose between two mounting sizes. The participants were randomly assigned to have the fingertip as the first stimulation location and the forearm as the second or vice versa to avoid learning bias. Participants wore headphones playing white noise throughout the session to prevent any additional information about the stimulation level other than somatosensory cues (e.g., noises from the pump).

At the end of the experiment, participants completed a quantitative evaluation using a seven-point Likert scale survey, consisting of ten questions about the system and the experimental tasks (control questions). The questions followed what was proposed by ref. [40]. The questionnaire assessed the comfort and quality of the experimental setup, the perceived performance, and the participant's engagement with the interface and feedback on the usage over a longer period (for full questionnaire see Table S2, Supporting Information).

Testing Protocol: User Study—Participants with Transradial Amputation: Three male individuals with transradial amputation (mean age 51.3 ± 13.6 years, right-hand amputation) participated in a single-session trial. Before the experiments, participants were asked if they were experiencing any limb or phantom pain. The 25 mm TPU actuator, specifically designed for mounting beneath the prosthetic socket (see Figure 1B), therefore having a long inlet that could be placed under the socket without being uncomfortable as a PVC tube would be, was positioned on areas of the residual limb that, when stimulated, evoked a phantom hand sensation in the missing limb (see Figure 4A). To identify these locations systematically, we followed the procedure defined in ref. [17], where a grid was applied to the residual limb, with each square assigned a number and letter. The phantom hand map was then defined by repeatedly probing each square with a round-tipped pencil. We furthermore aimed to activate the confirmed phantom sensation using a Monofilament kit (calibrated set for evaluation of tactile sensitivity). The small diameter of the filament activated the phantom sensations for two of the three participants only at a very high threshold (>15 g), basically puncturing the skin.

© 2025 The Author(s). Advanced Intelligent Systems published by Wiley-VCH GmbH

26404567, 0, Downloaded from https://advanced.onlinelibrary.wiley.com/doi/10.1002/aisy.202500262 by CochraneItalia, Wiley Online Library on [18/06/2025]. See the Terms and Conditions (https://onlinelibrary.wiley.com/terms-and-conditions) on Wiley Online Library for rules of use; OA articles are governed by the applicable Creative Commons License

Locations covered by electrodes used for controlling the prosthesis were excluded. Additionally, preference was given to skin spots that corresponded to the fingertips on the palmar side of the phantom hand, as these areas are most frequently involved in daily interactions with the environment. The 25 mm actuator was positioned at the predefined location on the residual limb and secured using standard medical tape. The amputee was then instructed to don the inner liner (ThermoLyn, Ottobock SE & Co. KGaA) as they normally would when mounting the prosthesis over the stump. Before the beginning of the tests, the actuator was gradually inflated up to a maximum pressure of 60 kPa, with continuous confirmation from the participant to ensure that the stimulation range did not cause any discomfort or pain. The experiments were conducted in a closed and quiet room. During the experiment, the participants sat comfortably next to the stimulation device, located on a separate table, to prevent vibration cues (see setup in Figure S8, Supporting Information). Participants wore headphones playing white noise throughout the session to prevent any additional information about the stimulation level other than somatosensory cues (e.g., noises from the pump).

Testing Protocol: User Study—Just Noticeable Difference Threshold Test: The JND was determined using the two-alternative forced choice (2AFC) method of constant stimuli.[53] In each trial, participants received two stimuli transmitted by the soft actuator in contact with the skin. Each pair consisted of a RS, and a CS. Following [54], the stimulation values were chosen so that the largest stimulus would almost always be judged greater than the RS, and the smallest CS would almost always be perceived lower than the RS. The predefined set of CS values was defined as 10, 22.5, 35, 47.5, and 60 kPa. The RS was set to 35 kPa. The total number of CS levels and repetitions was chosen as a trade-off between the precision of the estimated discrimination threshold and the duration of the experiment, as the latter could impact the participant's mental load and, thus, their performance. With five CS stimulation levels and twenty repetitions for each, the test consisted of 100 trials. The trapezoidal-shaped stimuli had a rise time of 250 ms and a stimulus duration of 1 s. The pause between the stimuli pair lasted 2 s (0 kPa), leading to a total test duration that was less than 15 min for each location. During each stimuli pair presentation, the order of the RS and CS was equally randomized. To familiarize the participants with the stimulation levels that would occur during the main experiment, the stimuli levels were presented twice in ascending order before the start of the measurement. Participants were asked if they experienced any discomfort. In addition, it was assured that any noise coming from the system was covered by the headphones. After the familiarization, the participants were presented with 100 randomized stimuli pairs. After each stimulus pair presentation, the participant reported which stimulus was perceived as stronger by selecting either stimulus 1 (first) or stimulus 2 (second) on a touchscreen. The participants were unaware that the paired values also included RS equal to CS. They were instructed to decide even if the levels were perceived as equal. The proportion of "stronger" (CS $>$ RS) responses was calculated for each stimulus level. For the cases where RS was compared against itself, a predefined vector was used to indicate if the first stimulus or the second one was considered as RS or CS. The vector contained 20 elements, half being the first stimulus and half being the second stimulus, in a randomized order. Using MATLAB (R2023b, Mathworks, USA) curve fitting toolbox, a psychometric function was fitted to the participant data (sigmoid, logistic using nonlinear least squares estimation). The JND was calculated for each participant using the point of subjective equality (PSE, the intensity value for 0.5 on the fitted psychometric function) and the intensity values at the 0.25 and 0.75 points on the psychometric function. Following,[54] the upper difference threshold was defined as the difference between the PSE and the 0.75 point, and the lower difference threshold as the difference between the PSE and the 0.25 point. The average of these two thresholds was taken as the difference threshold for the RS.[55] The overall JND was calculated as the mean JND between all able-bodied participants for the forearm and fingertip, as well as for the overall JND by the amputees.

Testing Protocol: User Study—Perception-Matching Test: In this test, a subgroup of five able-bodied participants (1 woman, 4 men, aged 26.6 ± 2.4 years, 4 right-handed) interacted with matched pairs of real and virtual rough surfaces. The experiment design included the rendering of three real surfaces: one smooth, and two sinusoidal with 1 and 4 mm spatial period (3D printed using Grey-Pro Resin, Formlabs, USA). The sinusoidal plates had a ridge height of 0.3 mm, and a ridge width of 0.4 mm, with a total plate length of 80 mm (values taken from refs. [32,55]). At the beginning of the test, the participants were introduced to the real plates, while staying unaware of the stimulation patterns provided by the system and the amount of them (no training was performed). To improve the roughness illusion, the interaction with the virtual surface was designed in an active manner. Therefore, the participant started the stimulation by using a haptic slider, designed for the experiment and consisting out of two force sensitive resistor, FSR (FSR07C, Ohmite, USA), 80 mm distant. The rendering was delivered via the soft actuator on the nondominant hand. The participants were instructed to slide on the one side along the haptic slider with the stimulated fingertip and simultaneously on the other side on the real plate (see Figure 3B). The participants were further instructed to slide the 80 mm length within 2 s, leading to a sliding velocity ν of 40 mm s^{-1} which is within the normal surface exploration speed.[32] Following the relation for the frequency f of vibration $f = \nu/\lambda$ (with the velocity ν and the spatial period λ),[56] this experimental parameters resulted in three rendering frequencies, aimed to match the three real surfaces: smooth, 1, 4 mm (0, 40 and 10 Hz). All stimuli were delivered with a baseline pressure of 10 kPa, while the amplitude of the sinusoidal vibration was set to 5 kPa for 40 Hz and 4 kPa for 10 Hz. The experiment consisted of three steps, one for each real surface plate. Within each step, the three virtual surfaces were presented five times against the real plate. Participants were able to repeat the stimulation until they decided for a similarity rating using verbal labels on a touchscreen (not at all, little bit, middle, very much and fully,).[55] The participants wore headphones, playing white noise throughout the session. The similarity rating was used to calculate the matching score, and then grouped as "same", i.e., when virtual stimuli matched the real surface, and as "diff", i.e., when virtual stimuli did not match the real surface (e.g., smooth surface but 1 mm virtual stimulus). Given the three possible stimuli (smooth, 1 and 4 mm) in the case of "diff," the ratings of the two remaining conditions were combined.

Testing Protocol: User Study—Intensity Classification Test: An intensity classification test was conducted with three participants with transradial amputations. The test aimed to evaluate their ability to distinguish and correctly classify the intensity of three stimuli. To do so, the participants were tasked with categorizing tactile stimuli delivered at three pressure levels: 10, 35, and 60 kPa (low, medium, and high). The stimuli had a rising time of 250 ms and a duration of 1 s. To familiarize the participants with the stimulation levels that would occur during the experiment, the stimuli levels were presented twice in ascending order before the start of the measurement.

During the experiment, each of the three levels were presented 20 times in a randomized order. During each trial, participants classified the perceived intensity of the stimulus into one of three predefined categories corresponding to the pressure levels (low, medium, and high). With three possible categories, the chance level for correct classification was 33.3%. Additionally, participants labeled their sensations using the terms "Pressure," "Touch," "Vibration," "Tingling," "Movement," "Discomfort," and "Undefined," based on.[38] If none of the labels matched their sensation, they selected "Undefined."

Supporting Information

Supporting Information is available from the Wiley Online Library or from the author.

Acknowledgements

This work was supported by the NEXTGENERATIONEU and Ministero dell'Università e della Ricerca THE (IECS00000017)—Tuscany Health Ecosystem (DN. 1553 11.10.2022) and project MNESYS (PE0000006)—A Multiscale Integrated Approach to the Study of the Nervous System in

© 2025 The Author(s). Advanced Intelligent Systems published by Wiley-VCH GmbH

26404567, 0, Downloaded from https://advanced.onlinelibrary.wiley.com/doi/10.1002/aisy.202500262 by CochraneItalia, Wiley Online Library on [18/06/2025]. See the Terms and Conditions (https://onlinelibrary.wiley.com/terms-and-conditions) on Wiley Online Library for rules of use; OA articles are governed by the applicable Creative Commons License

Health and Disease (DN. 1553 11.10.2022), and by the Italian National Institute for Insurance against Accidents at Work (INAIL Centro Protesi, Vigorso di Budrio, Bologna, Italy) within the PR23-PAS-P2 BioInterNect project.

Open access publishing facilitated by Scuola Superiore Sant'Anna, as part of the Wiley - CRUI-CARE agreement.

Conflict of Interest

The authors declare no conflict of interest.

Author Contributions

Hanna Scherer: conceptualization: (equ]al); data curation: (lead); formal analysis: (lead); investigation: (lead); methodology: (equal); writing—original draft: (equal). **Francesco Iberite**: conceptualization: (equal); data curation: (equal); investigation: (equal); methodology: (equal); software: (lead); writing—original draft: (equal). **Giulia Caserta**: writing—review and editing: (supporting). **Nicolo Boccardo**: writing—review and editing: (supporting). **Jacopo Carpaneto**: writing—review and editing: (supporting). **Emanuele Gruppioni**: writing—review and editing: (supporting). **Silvestro Micera**: conceptualization: (equal); funding acquisition: (lead); methodology: (equal); supervision: (equal); writing—original draft: (lead). **Tommaso Proietti**: conceptualization: (equal); methodology: (equal); supervision: (lead); visualization: (equal); writing—original draft: (equal). **Silvestro Micera** and **Tommaso Proietti** contributed equally to this work.

Data Availability Statement

The data that support the findings of this study are available from the corresponding author upon reasonable request.

Keywords

human–machine interfaces, multimodal feedback, sensory feedback, soft robotics, wearable haptics

Received: March 5, 2025
Revised: April 30, 2025
Published online:

[1] E. P. Gardner, J. H. Martin, Coding of Sensory Information, **2010**, https://api.semanticscholar.org/CorpusID:16301988, (accessed: September, 2024).
[2] A. Gerald, S. Russo, *Nat. Rev. Mater.* **2024**, *9*, 86, https://doi.org/10.1038/s41578-024-00653-6.
[3] R. V. Patel, S. F. Atashzar, M. Tavakoli, *Proc. IEEE* **2022**, *110*, 1012, https://doi.10.1109/JPROC.2022.3180052.
[4] X. Yu, Z. Xie, Y. Yu, et al., *Nature* **2019**, *575*, 473, https://doi.org/10.1038/s41586-019-1687-0.
[5] P. Svensson, U. Wijk, A. Björkman, C. Antfolk, *Expert Rev. Med. Devices* **2017**, *14*, 439, https://doi.org/10.1080/17434440.2017.1332989.
[6] I. Nisky, T. R. Makin, *Sci. Adv.* **2024**, 10, https://doi.10.1126/sciadv.adq6290.
[7] V. Shen, T. Rae-Grant, J. Mullenbach, C. Harrison, C. Shultz, in *Proc. of the 36th Annual ACM Symp. on User Interface Software and Technology, Association for Computing Machinery*, New York, NY, USA, Article 8 **2023**, pp. 1–20, https://doi.org/10.1145/3586183.3606771.
[8] S. Gallo, C. Son, H. J. Lee, H. Bleuler, I.-J. Cho, *Sens. Actuators A Phys.* **2015**, *236*, 180, https://doi.org/10.1016/j.sna.2015.10.048.
[9] S. Fani, K. Di Blasio, M. Bianchi, M. G. Catalano, G. Grioli, A. Bicchi, *IEEE Robot. Autom. Lett.* **2019**, *4*, 926, doi:10.1109/LRA.2019.2894380.
[10] P. Preechayasomboon, E. Rombokas, *Front Virt. Real.* **2021**, *2*, https://doi.org/10.3389/frvir.2021.738613.
[11] F. Barontini, *IEEE Trans. Haptics* **2023**, *16*, 760, https://doi.org/10.1007/978-3-031-70539-7_3.
[12] M. Buist, S. Damercheli, M. T. N. Truong, A. Sanna, E. Mastinu, M. Ortiz-Catalan, *IEEE Trans. Biomed. Circuits Syst.* **2023**, *1*, doi:10.1109/TBCAS.2023.3271821.
[13] B. Jumet, Z. A. Zook, D. Xu, N. Fino, A. Rajappan, M. W. Schara, J. Berning, N. Escobar, M. K. O'Malley, D. J. Preston., in *2022 IEEE 5th Inter. Conf. on Soft Robotics, RoboSoft 2022,* IEEE, Piscataway, NJ **2022**, pp. 741–746.
[14] M. F. Simons, K. Manaswi Digumarti, N. Hao Le, H. Chen, S. Correia Carreira, N. S. S. Zaghloul, R. Suphapol Diteesawat, M. Garrad, A. T. Conn, C. Kent, J. Rossiter, *IEEE Robot. Autom. Lett.* **2021**, *6*, 3311, doi:10.1109/LRA.2021.3064269.
[15] R. Rangwani, H. Park, *J. Neuroeng. Rehabil.* **2021**, *18*, https://doi.org/10.1186/s12984-021-00870-y.
[16] G. Gu, N. Zhang, H. Xu, S. Lin, Y. Yu, G. Chai, L. Ge, H. Yang, Q. Shao, X. Sheng, X. Zhu, X. Zhao, *Nat. Biomed. Eng.* **2023**, *7*, 589, https://doi.org/10.1038/s41551-021-00767-0.
[17] F. Iberite, J. Muheim, O. Akouissi, A. Gallo, G. Rognini, F. Morosato, A. Clerc, M. Kalff, E. Gruppioni, S. Micera, S. Shokur, *Science* **2023**, *380*, 731, doi:10.1126/science.adf6121.
[18] B. Zhang, M. Sra, in *Proc. of the 27th ACM Symp. on Virtual Reality Software and Technology, VRST*, Association for Computing Machinery, New York, NY, USA **2021**, https://doi.org/10.1145/3489849.3489857.
[19] G. Frediani, F. Carpi, *Sci. Rep.* **2020**, *10*, https://doi.org/10.1038/s41598-020-77591-0.
[20] W. Guo, Y. Hu, Z. Yin, H. Wu, Special Issue:*Green Electronics*, John Wiley and Sons Inc., Hoboken NJ **2022**, https://doi.org/10.1002/admt.202100452.
[21] R. E. Fan, M. O. Culjat, C. King, M. L. Franco, R. Boryk, J. W. Bisley, E. Duston, W. S. Grundfest, *IEEE Trans. Neural Syst. Rehabil. Eng.* **2008**, *16*, 270, doi:10.1109/TNSRE.2008.920075.
[22] F. Clemente, M. D'Alonzo, M. Controzzi, B. B. Edin, C. Cipriani, *IEEE Trans. Neural Syst. Rehabil. Eng.* **2016**, *24*, 1314, doi:10.1109/TNSRE.2015.2500586.
[23] Y. H. Jung, J. Yoo, A. Vazquez-Guardado, J. Kim, J. Kim, H. Luan, M. Park, J. Lim, H. Shin, C. Su, R. Schloen, J. Trueb, R. Avila, J. Chang, D. S. Yang, Y. Park, H. Ryu, H. Yoon, G. Lee, H. Jeong, J. U. Kim, A. Akhtar, J. Cornman, T. Kim, Y. Huang, J. A. Rogers, *Nat Electron* **2022**, *5*, 374, https://doi.org/10.1038/s41928-022-00765-3.
[24] K. A. Kaczmarek, J. G. Webster, P. Bach-Y-Rita, W. J. Tompkins, *IEEE Trans. Biomed. Eng.* **1991**, *38*, 1, doi:10.1109/10.68204.PMID:2026426.
[25] C. Antfolk, C. Balkenius, B. Rosén, G. Lundborg, F. Sebelius, *J. Plast. Surg. Hand. Surg.* **2010**, *44*, 50, https://doi.org/10.3109/02844310903259090.
[26] K. Kim, J. E. Colgate, J. J. Santos-Munné, A. Makhlin, M. A. Peshkin, *IEEE/ASME Trans. Mechatronics* **2010**, *15*, 27, doi:10.1109/TMECH.2009.2013944.
[27] H. Zhao, et al., *Soft Robot.* **2020**, *7*, 451, https://doi.org/10.1089/soro.2019.011.
[28] K. Song, et al., *Sci. Rep.* **2019**, *9*, https://doi.org/10.1038/s41598-019-45422-6.

© 2025 The Author(s). Advanced Intelligent Systems published by Wiley-VCH GmbH

26404567, 0, Downloaded from https://advanced.onlinelibrary.wiley.com/doi/10.1002/aisy.202500262 by CochraneItalia, Wiley Online Library on [18/06/2025]. See the Terms and Conditions (https://onlinelibrary.wiley.com/terms-and-conditions) on Wiley Online Library for rules of use; OA articles are governed by the applicable Creative Commons License

[29] M. W. M. Tan, H. Wang, D. Gao, P. Huang, P. S. Lee, *Roy. Soc. Chem.* **2024**, https://doi.org/10.1039/d3cs01017a.
[30] W.-M. Zhang, G. Meng, D. Chen, *Sensors* **2007**, *7*, 760-96, https://doi.org/10.3390/s7050760.
[31] E. M. Young, A. H. Memar, P. Agarwal, N. Colonnese, in *2019 IEEE World Haptics Conference (WHC)*, IEEE, Piscataway, NJ. **2019**, p. 55. https://doi.org/10.1109/WHC.2019.8816075.
[32] H. A. Sonar, J.-L. Huang, J. Paik, *Adv. Intell. Syst.* **2021**, *3*, https://doi.org/10.1002/aisy.202000168.
[33] M. Zhu, et al. in *Proc. of the 2020 CHI Conf. on Human Factors in Computing Systems*, ACM, New York, NY **2020**, pp. 1–12, https://doi.org/10.1145/3313831.3376333.
[34] B. Jumet, Z. A. Zook, A. Yousaf, A. Rajappan, D. Xu, T. Faye Yap, N. Fino, Z. Liu, M. K. O'Malley, D. J. Preston, *Device* **2023**, *1*, https://doi.org/10.1016/j.device.2023.100059.
[35] L. Ekman, E. Lindholm, E. Brogren, L. B. Dahlin, *PLoS One* **2021**, *16*, https://doi.org/10.1371/journal.pone.0249461.
[36] U. Tanriverdi, G. Senesi, T. Asfour, H. Kurt, S. L. Smith, D. Toderita, J. Shalhoub, L. Burgess, A. M. J. Bull, F. Güder, *Nat. Commun.* **2025**, *16*, https://doi.org/10.1038/s41467-025-57634-8.
[37] B. Berglund, T. Lindvall, D. H. Schwela, *Noise Vibr. Worldwide* **2000**, *31*, 24, https://doi.org/10.1260/0957456001497535.
[38] L. H. Kim, R. S. McLeod, Z. H. T. Kiss, *J. Neural Eng.* **2018**, *15*, https://doi.org/10.1088/1741-2552/aa966a.
[39] A. Talhan, H. Kim, S. Jeon, *IEEE Access* **2020**, *8*, 957, doi:10.1109/ACCESS.2019.2961430.
[40] F. Barontini, M. G. Catalano, G. Grioli, M. Bianchi, A. Bicchi, *IEEE Robot. Autom. Lett.* **2021**, *6*, 1785-1792, doi:10.1109/LRA.2021.3060432.
[41] M. S. Hashem, J. B. Joolee, W. Hassan, S. Jeon, *Appl. Sci.* **2022**, *12*, https://doi.org/10.3390/app12010175.
[42] J. J. Huaroto, E. Suarez, H. I. Krebs, P. D. Marasco, E. A. Vela, *IEEE Robot. Autom. Lett.* **2019**, *4*, 17, doi:10.1109/LRA.2018.2874379.
[43] G. Valle, A. Mazzoni, F. Iberite, E. D'Anna, I. Strauss, G. Granata, M. Controzzi, F. Clemente, G. Rognini, C. Cipriani, T. Stieglitz, F. M. Petrini, P. M. Rossini, S. Micera, *Neuron* **2018**, *100*, 37, https://doi.org/10.1016/j.neuron.2018.08.033.
[44] C. Antfolk, A. Björkman, S. Frank, F. Sebelius, G. Lundborg, B. Rosen, *J. Rehabil. Med.* **2012**, *44*, 702, https://doi.org/10.2340/16501977-1001.
[45] S. J. Bensmaia, D. J. Tyler, S. Micera, *Nat. Res.* **2023**, https://doi.org/10.1038/s41551-020-00630-8.
[46] N. Gozzi, L. Chee, I. Odermatt, S. Kikkert, G. Preatoni, G.. Valle, N. Pfender, F. Beuschlein, N. Wenderoth, C. Zipser, S. Raspopovic, *Nat. Commun.* **2024**, *15*, https://doi.org/10.1038/s41467-024-55152-7.
[47] G. Valle, F. M. Petrini, I. Strauss, F. Iberite, E. D'Anna, G. Granata, M. Controzzi, C. Cipriani, T. Stieglitz, P. M. Rossini, A. Mazzoni, A. Raspopovic, S. Micera, *Sci. Rep.* **2018**, *8*, https://doi.org/10.1038/s41598-018-34910-w.
[48] D. W. Tan, M. A. Schiefer, M. W. Keith, J. R. Anderson, J. Tyler, D. J. Tyler, *Sci. Transl. Med.* **2014**, *6*, https://doi.org/10.1126/scitranslmed.3008669.
[49] B. Stephens-Fripp, G. Alici, R. Mutlu, IEEE Access, Piscataway NJ **2018**, *6*, 6878, https://doi.org/10.1109/ACCESS.2018.2791583.
[50] C. du Pasquier, L. Tessmer, I. Scholl, L. Tilton, T. Chen, S. Tibbits, A. Okamura, *Sci. Robot.* **2024**, *9*, doi:10.1126/scirobotics.ado3887.
[51] A. Handler, D. D. Ginty, *Nat. Res.* **2021**, https://doi.org/10.1038/s41583-021-00489-x.
[52] G. Corniani and H. P. Saal, *J. Neurophysiol.* **2020**, *124*, 1229, https://doi.org/10.1152/jn.00313.2020.
[53] W. H. Ehrenstein, A. Ehrenstein, *Psychophysical Methods*, in *Modern Techniques in Neuroscience Research*, Springer, Berlin, Heidelberg **1999**, https://doi.org/10.1007/978-3-642-58552-4_43.
[54] L. A. Jones, H. Z. Tan, *IEEE Trans. Haptics* **2013**, *6*, 268, doi:10.1109/TOH.2012.74.
[55] U. Alican Alma, R. Rosenkranz, M. Ercan Altinsoy, *IEEE Trans. Haptics* **2023**, *16*, 204, https://doi.org/10.1109/TOH.2023.3252669.
[56] M. Konyo, T. Maeno, A. Yoshida, S. Tadokoro, Presented at World Haptics Conf., Pisa, Italy, **2005**, pp. 609-610, doi:10.1109/WHC.2005.113.

© 2025 The Author(s). Advanced Intelligent Systems published by Wiley-VCH GmbH

26404567, 0, Downloaded from https://advanced.onlinelibrary.wiley.com/doi/10.1002/aisy.202500262 by CochraneItalia, Wiley Online Library on [18/06/2025]. See the Terms and Conditions (https://onlinelibrary.wiley.com/terms-and-conditions) on Wiley Online Library for rules of use; OA articles are governed by the applicable Creative Commons License